Electronic Supplementary Information

Growth of Single Crystal, Oriented SnO_2 Nanocolumn Arrays by Aerosol Chemical Vapor Deposition (ACVD)

Kelsey Haddad[1], Ahmed A. Abokifa[1], Shalinee Kavadiya[1], Tandeep S. Chadha[1], Pranav Shetty[1,†], Yang Wang[1], John Fortner[1], Pratim Biswas[1*]

[1]Department of Energy, Environmental & Chemical Engineering
Washington University in St. Louis
St. Louis, MO-63130, USA

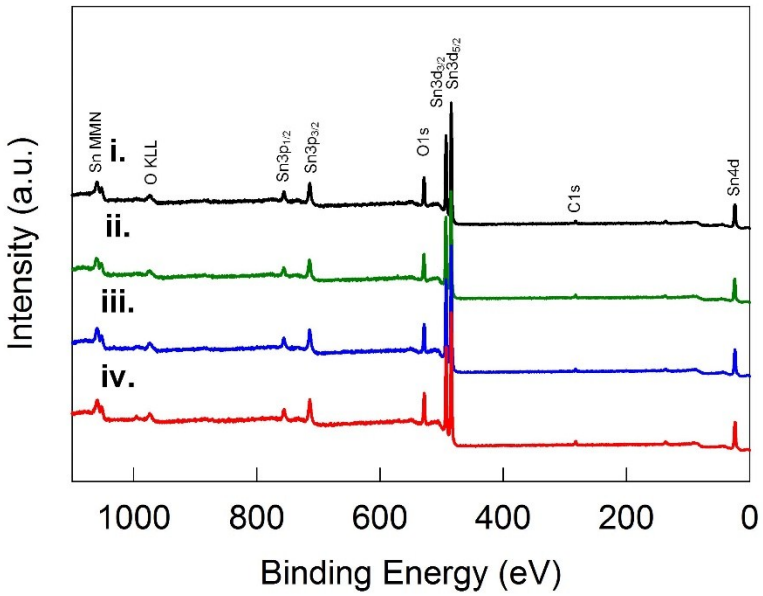

Figure S1. XPS spectrum confirming the purity of the SnO_2 columnar thin films grown at (i) 450 °C, 500 °C, 550 °C, 600 °C.

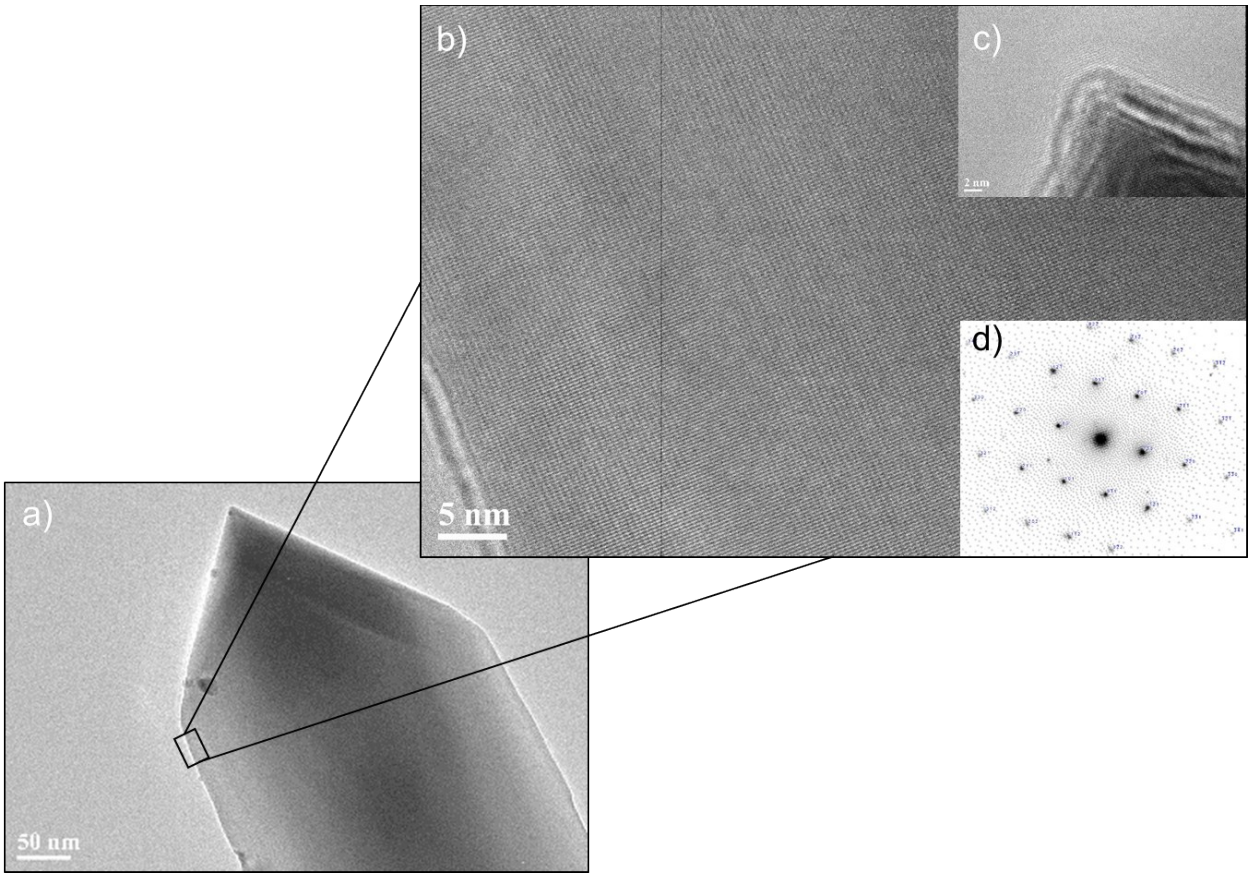

Figure S2. TEM image of a single column. b-c) HR-TEM image of the nanoneedle structure and d) SAED pattern confirming an individual needle is a single crystal.

Grazing-Incidence Small-Angle X-ray Scattering

The horizontal and vertical linecuts provide information on the horizontal and vertical dimension of the nanocolumn, respectively. The horizontal linecuts provide information on horizontal dimensions of the nanocolumns. Using the Guinier law and fitting the curve along the Guinier region of 1D wave vector for linecut at q_z = 0.013-0.023 Å^{-1}, two characteristic dimensions were found to be 1.94 nm and 8 nm. Similar curve fitting was done in the Guinier region for the horizontal linecut at q_z = 0.027-0.037 Å^{-1}, and the corresponding dimension is 2.63 nm. Vertical linecut was made at q_y = 0.03 Å^{-1} and 0.062 Å^{-1} to extract the dependence of intensity on q_z. Both the linecuts represents the similar 1D I-q_z wave vector and have a peak around 0.015 Å^{-1} corresponding to vertical dimension of 39 nm.

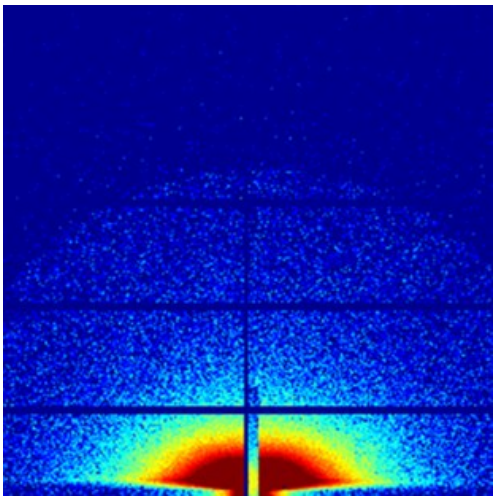

Figure S3. 2-D GISAXS pattern for samples prepared at 450 ˚C (Test 4)

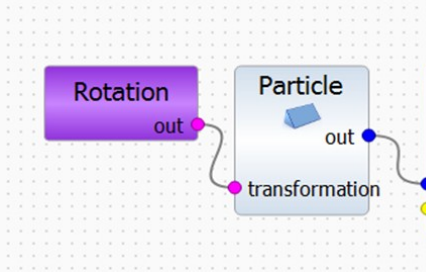

Figure S4. Schematic of the model built in the software BornAgain.

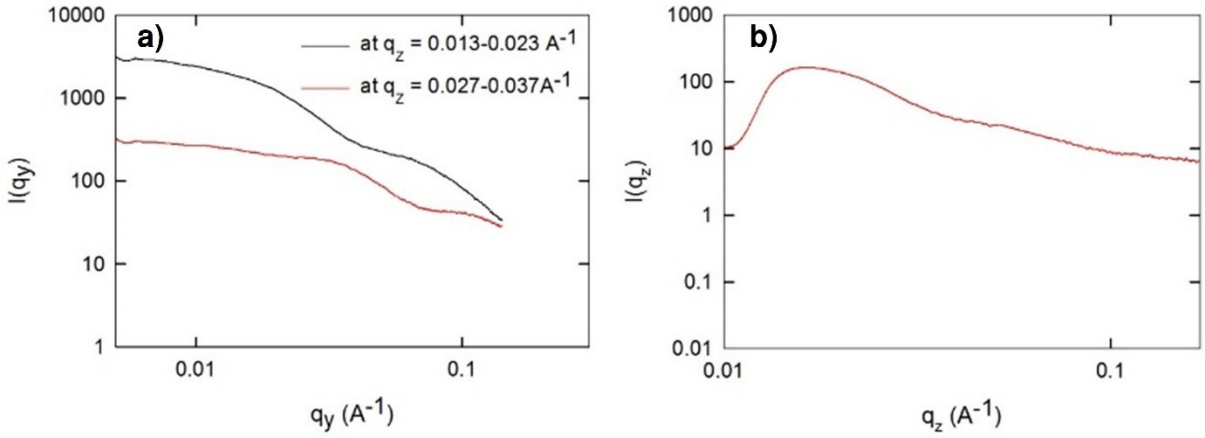

Figure S5. 1-D I vs q curve generated by (a) horizontal linecut at two different regions of q_z – 0.013-0.023 $Å^{-1}$ (red curve) and 0.027-0.037 $Å^{-1}$ (black curve) (b) vertical linecut on the 2-D scattering pattern of SnO_2 deposited at 600˚C.

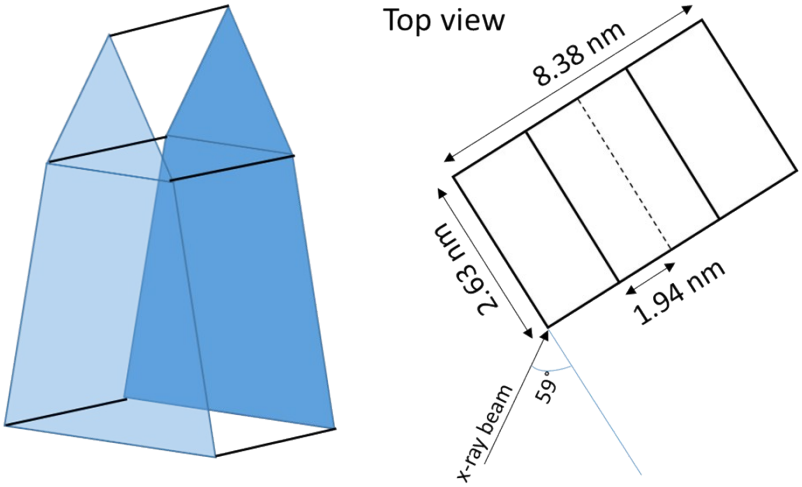

Figure S6. Schematic of 3-D geometry of the needle estimated by simulation in BornAgain and SEM image.

Density functional theory methods

The Sn 4d, Sn 5s, Sn 5p, as well as the O2s and O2p states were treated as valence states. We used the standard ultra-soft pseudopotentials included in the VASP package. Between the cores, the wave functions are expanded into plane waves up to a cut- off energy of 520 eV. To sample the Brillouin zone, the k-meshes were generated automatically using the Monkhorst–Pack (MP) method. In the case of bulk SnO_2, the Brillouin zone (BZ) integration is replaced by a sum over 5×5×7 (MP) k-points, while for the surface calculations, we used 7×5×1 MP points for the (110) surface, and 5×5×1 MP points for the (101) and the (211) surfaces, which is consistent with what previous researchers have used for similar types of calculations.[1] In addition, we conducted separate test runs to guarantee the convergence of the total energies for the bulk structure and the stoichiometric surface slabs with the chosen number of k-points to a threshold of 1 meV/cell. In order to determine the ground state atomic geometries, we used a conjugate-gradient algorithm to

relax the positions of the atoms until the total forces on each ion are smaller than 0.02 eV/Å, and employing a total energy convergence of 10^{-5} eV in the self- consistency cycle.

The surfaces were modeled as slabs cut from the fully relaxed bulk structure with an imposed vacuum layer of 15 Å. The number of atomic layers considered in the stoichiometric surface slabs is 7 layers, where each layer has six ions (Sn_2O_4) per repeating unit. Previous studies found that five and seven layers are required to achieve convergence for the (110) and the (101) surface slabs.[2] In separate calculations, the convergence of the surface energy was checked with the number of atomic layers for the stoichiometric (211) surface slab and we concluded that seven layers are sufficient to achieve convergence in the calculated surface energy within one meV/Å.[2]

Description of the atomic layers for the stoichiometric (110) and (101) surfaces can be found elsewhere[3]. For the high index (211) surface, each atomic layer can be best formulated as [O(2-)-O(2-)-Sn_2(8+)- O(2-)-O(2-)], with the surface tin layer consisting of alternating rows of four- and five-fold coordinated tin atoms. For the five-fold tin, one of the equatorial oxygens is missing, while one equatorial and one apical oxygens are missing from the coordination polyhedron of the four-fold tin atom. This gives rise to two layers of oxygen atoms lying on each side – above and below— of the tin layer at distances equivalent to the equatorial and apical Sn-O bond lengths, respectively. The topmost row consists of under-saturated oxygen atoms that are two-fold coordinated and bonded to the four- and five-fold tin atoms, and thus can be considered to occupy “bridging” locations. The bottommost row consists of three-fold coordinated oxygens with both the topmost and the bottommost oxygen rows laying in the apical sites of the five-fold tin. The two oxygen rows directly sandwiching the surface tin layer are two-fold coordinated, and both lay in the equatorial sites of the five-fold tin.

The partially reduced surface of the (110) facet was constructed by consistently removing the top layer of the bridging oxygen atoms creating a surface layer of alternating rows of four- and five-fold Sn atoms and in-plane oxygen atoms, which corresponds to a surface layer with the Sn_2O_3 composition. The fully reduced (110) surface was constructed by further removing alternating rows of the in-plane oxygen atoms, which creates a surface layer of Sn^{2+} with three-fold co-ordination (Fig S6). For the (101) surface, the partially and fully reduced surface stoichiometries are created by either removing alternating rows or all rows of the bridging oxygen atoms, which creates a surface layer of tin atoms that are four-fold or three-fold coordinated, respectively. The partially reduced (211) surface was constructed by removing the topmost layer of the bridging two-fold oxygen atoms, which creates a mixed layer of three-and four-fold coordinated tin atoms, while removing the following layer of oxygen atoms creates the fully reduced surface, with threefold coordinated Sn^{2+} atoms.

Our results for the lattice constants of the ground-state rutile tetragonal SnO_2 bulk structure ($P4_2/mnm$ space group) with the DFT-PBE are: a=b=4.818 Å and c=3.243 Å. The employed PBE functional over-estimated the experimental results of a=b=4.7367Å, and c=3.1855 Å with a relative error that is less than 2%, which is consistent with what previous researchers calculated for the bulk structure.[4] We also tested the local-density approximation (LDA) and the hybrid Heyd-Scuseria-Ernzerhof (HSE06) XC functionals for the bulk structure, and the results of both functionals were more consistent with the experimental parameters (LDA: a= 4.732 Å; c=3.196 Å, HSE06: a= 4.740 Å; c=3.180 Å). However, we employed the PBE functional for the surface slab calculations because the LDA is known to be inaccurate for such surface calculations[3] and the use hybrid HSE06 functional would be computationally inhibitive.

Dangling bond density of different crystal facets

The stoichiometric (110) surface facet of the rutile SnO_2 consists of alternating rows of six-fold coordinated and five-fold coordinated surface Sn atoms with one dangling bond that is perpendicular to the surface. However, on the stoichiometric (101) surface, all surface Sn atoms are coordinately unsaturated and located in five-fold coordinated sites with one dangling bond. The high index (211) surface exposes alternating layers of five-fold coordinated and four-fold coordinated surface Sn atoms with one and two dangling bonds, respectively. Therefore,

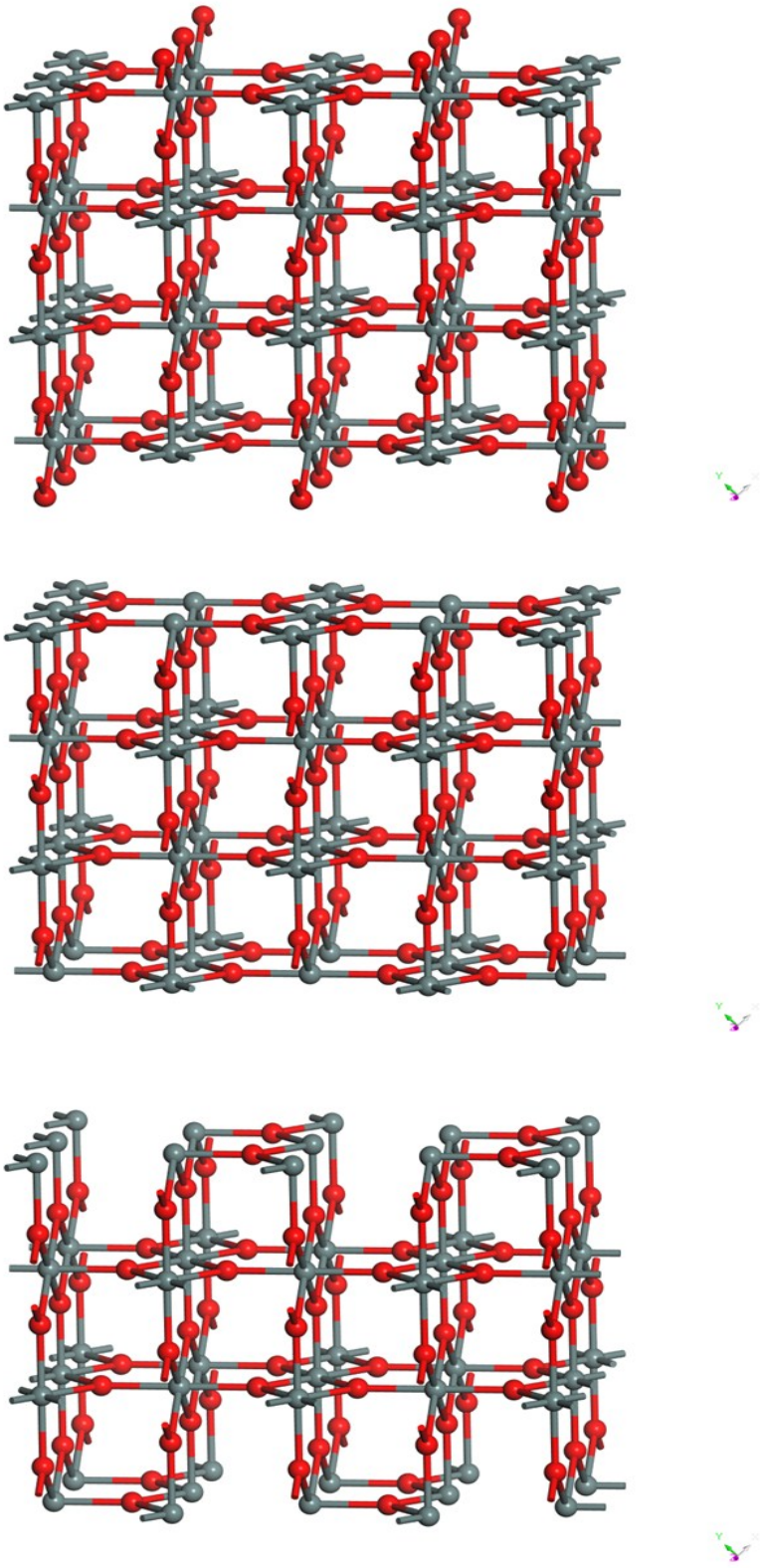

Figure S7. Ball and stick models of the stoichiometric, partially reduced, and fully reduced (110) surfaces.

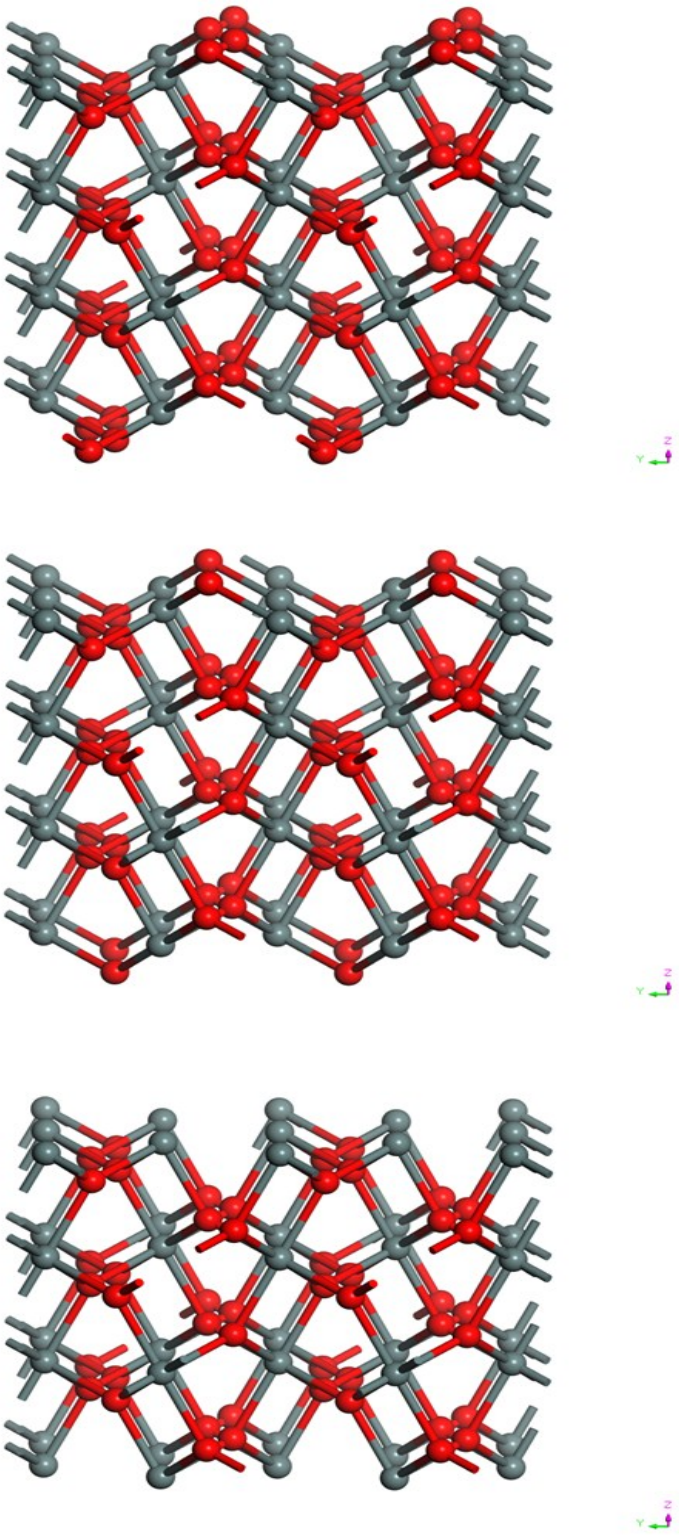

Figure S8. Ball and stick models of the stoichiometric, partially reduced, and fully reduced (101) surfaces.

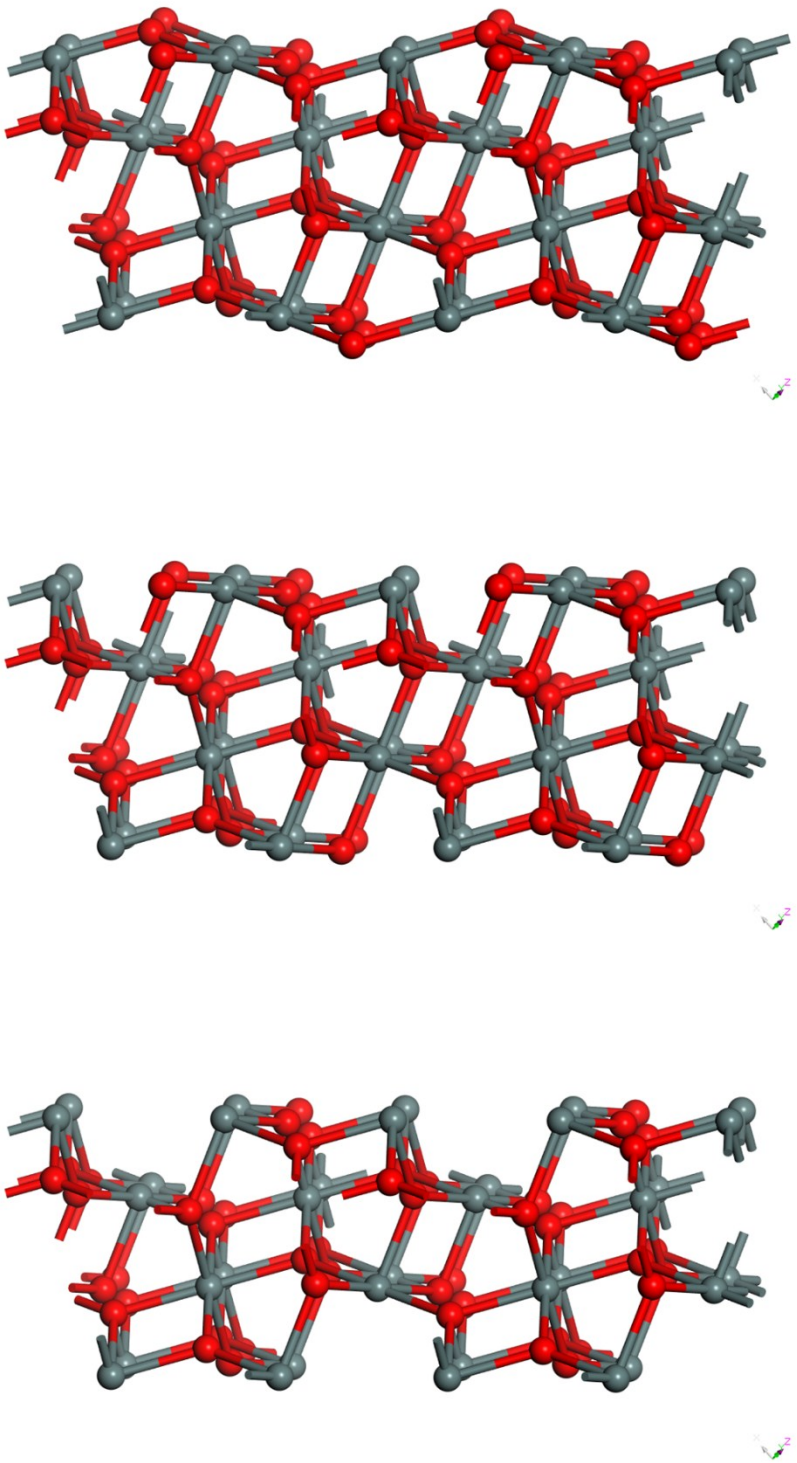

Figure S9. Ball and stick models of the stoichiometric, partially reduced, and fully reduced (211) surfaces.

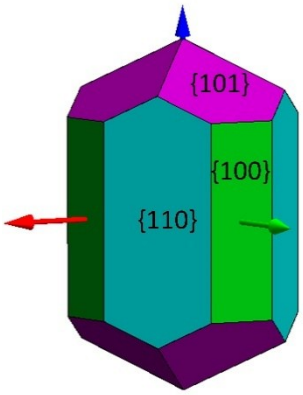

Figure S10. Wulff construction of the equilibrium crystal morphology of the seed particles formed in the gas phase and deposited on the substrate surface (300 K).

References

1. J. D. Prades, A. Cirera and J. R. Morante, *Journal of The Electrochemical Society*, 2007, **154**, H675-H680.
2. W. Bergermayer and I. Tanaka, *Applied Physics Letters*, 2004, **84**, 909.
3. J. Oviedo and M. Gillan, *Surface Science*, 2000, **463**, 93-101.
4. Y. Jiang, C. Xu and G. Lan, *Transactions of Nonferrous Metals Society of China*, 2013, **23**, 180-192.